Structural Engineering and Mechanics, *Vol. 73, No. 6 (2020) 715-724*
DOI: https://doi.org/10.12989/sem.2020.73.6.715

Experimental and numerical bending deflection of cenosphere filled hybrid (Glass/Cenosphere/Epoxy) composite

Harsh Kumar Pandey[1a], Himanshu Agrawal[2b], Subrata Kumar Panda[*3], Chetan Kumar Hirwani[4c], Pankaj V. Katariya[3d] and Hukum Chand Dewangan[3e]

[1]*Department of Mechanical Engineering, Dr. C.V. Raman Institute of Science & Technology, Bilaspur (C.G.), India*
[2]*Department of Mechanical Engineering, Government Engineering College, Jagdalpur, Chhattisgarh, India 494001*
[3]*Department of Mechanical Engineering, NIT Rourkela, Rourkela, Odisha, Sundergarh, India 769008*
[4]*Department Mechanical Engineering, National Institute of Technology Patna, Bihar, India, 800005*

(Received August 11, 2019, Revised October 19, 2019, Accepted November 22, 2019)

Abstract. The influence on flexural strength of Glass/Epoxy laminated composite curved panels of different geometries (cylindrical, spherical, elliptical, hyperboloid and flat) due to inclusion of nano cenosphere filler examined in this research article. The deflection responses of the hybrid structure are evaluated numerically using the isoparametric finite element technique and modelled mathematically via higher-order displacement structural kinematics. To predict the deflection values, a customised in-house computer code in MATLAB environment is prepared using the higher-order isoparametric formulation. Subsequently, the numerical model validity has been established by comparing with those of available benchmark solution including the convergence characteristics of the finite element solution. Further, a few cenosphere filled hybrid composite are prepared for different volume fractions for the experimental purpose, to review the propose model accuracy. The experimental deflection values are compared with the finite element solutions, where the experimental elastic properties are adopted for the computation. Finally, the effect of different variable design dependent parameter and the percentages of nano cenosphere including the geometrical shapes obtained via a set of numerical experimentation.

Keywords: experimental bending; hybrid composite; glass cenosphere; FEM, HSDT

1. Introduction

The laminated composite structural components are commonly utilized in the different modern field like marine, aeronautical and space structure, where the weight penalty is one of the major concern without compromising the strength and stiffness values. Further, to maintain as well as to improve the structural performances, varieties of filler materials also got the attentions for the hybridization new composite too. The research relevant to the mechanical characterisation of the advanced industrial composite construction including the hybrid structural component indicate the importance of filler materials for the specific application. In this regard, the glass nano cenospheres is one of the common filler materials with differently abled capability for the structural implementation. These cenospheres help the composite to improve the desirable properties without hampering weight due to its hollow geometry. Further, research related glass cenosphere filled with inert gas (Yung *et al.* 2009), indicates a considerable improvement in some unique properties (light weight, low thermal conductivity and low dielectric constant). The research related to the composite properties and subsequent application considering the glass cenospheres as a filler material are highlighted in the following subsection and to point-out the research gap.

Yung *et al.* (2009) investigated the effect of increasing fractions of hollow glass microsphere within epoxy composite and their influence on the dielectric properties. The effect of hollow glass microspheres on the mechanical properties and the curing behaviour of the hollow glass microsphere/bisphenol filled dicyanate ester composite (Wang *et al.* 2010). Wu *et al.* (2016) studied the preparation and the subsequent characterization of three-phase epoxy syntactic foam filled with carbon fiber reinforced hollow epoxy macrosphere and hollow glass microsphere. Zhang and Ma (2010) studied the effect of glutaric dialdehyde coupling agent on the properties of hollow carbon microsphere/phenolic resin syntactic foam under the mechanical loading. Zhang and Ma (2013) evaluated experimentally the effect of carbon nanofiber reinforcement on the mechanical properties of syntactic foams. Similarly, the effect of increasing weight percentages of the hollow glass microspheres on the dispersion state of single-walled carbon nanotube evaluated by Kang *et al.* (2017). The

*Corresponding author, Ph.D.. Associate Professor
E-mail: pandask@nitrkl.ac.in, call2subrat@gmail.com
[a] M. Tech, Research Scholar
E-mail: harsh25pandey@gmail.com
[b] Ph.D., Associate Professor
E-mail: himanshu.jglr@gmail.com
[c] Ph.D., Assistant Professor
E-mail: chetanhirwani111@gmail.com
[d] M. Tech, Research Scholar
E-mail: pk.pankajkatariya@gmail.com
[e] M. Tech, Research Scholar
E-mail: hukumdewangan@gmail.com

Copyright © 2020 Techno-Press, Ltd.
http://www.techno-press.com/journals/sem&subpage=7
ISSN: 1225-4568 (Print), 1598-6217 (Online)

tensile properties and the fracture mode of syntactic foams filled with glass microballoon due to the different volume fractions and densities of glass microballons reported by Gupta and Nagorny (2005). Liang and Li (2000) studied the effect of adding of filler content (A-glass beads) on the tensile properties of the glass-bead-filled polypropylene composite. Kumar *et al*. (2017) investigated the strength related properties and morphological behaviour of the lightweight high-strength hollow glass microspheres and bamboo fibre-based hybrid polypropylene composite. Li *et al.* (2013) presented the preparation and characterisation steps for various hollow glass microspheres filled poly (butylene succinate)/hollow glass microsphere (PBS/HGM) composite. Zhu *et al.* (2014) investigated the effect of volume fraction, density and surface modification of hollow glass microsphere filler on the thermal and dielectric properties of low-density polyethylene matrix composite. Wang *et al*. (2014) studied the effect of microsphere on the compressive behaviour of microsphere filled epoxy foam composite by optimizing the foaming temperature. The numerical finite element simulations are conducted for the sandwich composite skins made of hybrid glass-fibre/polymer-matrix composite with hollow glass microspheres foam filler by Corigliano *et al.* (2000) and verified with experimental test data. Similarly, the mechanical and the electrical properties for the high performance circuit boards reported by Kempf *et al.* (2000) using a pre-preg substrate contains uniformly distributed hollow glass microsphere filler of low dielectric constant. The infrared radiative properties of hollow glass microsphere filled polymer are studied (Dombrovsky *et al*. 2007) using the values of directional-hemispherical reflectance and transmittance under the wavelength ranging from 2.6 to 18 µm. The effect of hollow glass microsphere fillers and the addition of short fibres reinforcement on the binding behaviour of epoxy matrix composite presented by Ferreira *et al.* (2010). Arencon *et al.* (2006) investigated the fracture behaviour of glass microsphere filled polypropylene/poly (ethylene terephthalate-coisophthalate) blend-matrix composite and compared with that of the glass microsphere-filled polypropylene composite. Doumbia *et al*. (2015) used hollow microspheres to reduce the density of the bumper type of polypropylene components for the investigation of the high impact characteristics. Zidi *et al.* assumed a new mathematical expression for the kinematic modeling of the functional graded material (FGM) plate resting on elastic foundation to evaluate the transverse mechanical bending under the hygro-thermo mechanical loading. The study of finite element about a layered composite cylinder using the connection between macro and microstructure. Esmaeili *et al.* (2014) conducted the theoretical analysis of carbon nanotube reinforced pipes bending strength and the verified with experimental values for the application in the field of oil and gas industries. Additionally, the transverse bending, buckling and dynamic responses of composite structure including the nano-filler and the size effect have been investigated via different numerical and/or exact techniques by Kolahchi and his co-authors (Heydari *et al.* 2014, Kolahchi *et al*. 2015, Arani *et al*. 2016a, b, Kolahchi *et al.* 2019, Jassas *et al*. 2019, Amnieh *et al*. 2018, Hajmohammad *et al*. 2018a, 2b, 2018c). The nonlinear dynamic responses of functionally graded carbon nanotube-reinforced composite (FG-CNTRC) beam type structural component analysed by Asadi and Beheshti (2018) when exposed to axial supersonic airflow with elevated thermal environment. Bellifa *et al.* (2016) studied the bending and eigenvalues of the FG plate using a new first-order shear deformation polynomial theory (FOSDPT) considering the eccentricity of neutral surface position. The prestressed end-notched flexure system used by Szekrenyes (2010) instead of the mixed-mode bending for the delamination testing of composite component under the mixed-mode I/II condition to avoid the complex loading fixture. Similarly, the variational approach in association with Ritz method have been adopted for the analysis of bending, buckling and vibration responses of Timoshenko and Euler's beam type component using the nonlocal elasticity under the arbitrary boundary conditions (Ghannadpour 2013 and 2018). Ghannadpour and Alinia (2006) studied the large deflection analysis of rectangular FG plate under the pressure load considering von-Karman nonlinear strain theory. Ovesy and Ghannadpour (2006) utilized finite strip method for the computation of the large deflections of FG plate under the normal pressure loading. Taghizadeh *et al.* (2015) reported the finite element solutions of the beam bending deflections including the nonlocal integral elasticity.

The review reveals that attempt has been made in the past to study the structural responses (bending, vibration, buckling) via different solution techniques including the material type i.e., graded, laminated composite (with and without different filler). In addition, the major effort has also been made to improve the elastic material properties of laminated composite component by adding an extra amount of the filler and the relevant characterisation expressed in details. However, no study has been reported yet in the open articles regarding the numerical material model of hybrid laminated composite filled with glass cenosphere. Hence, the glass cenosphere filled laminated glass/epoxy composite has been modeled through a higher-order kinematic polynomial kinematic theory and their transverse mechanical bending responses also evaluated using the finite element approach. Moreover, the exactness of the proposed model verified with the own experimental data. It is important to mention that the numerical responses are obtained using the experimental elastic properties of in-house fabricated glass cenosphere filled glass/epoxy hybrid composite via hand-layup techniques. Based on the model validation, the proposed higher-order FE model explored to understand the effect design dependent parameters on the subsequent bending deflections by solving variable numerical examples. Finally, the increasing percentage of cenosphere in the hybrid composite configuration including the geometrical configurations on the stiffness characteristics are discussed in details.

2. Mathematical modelling

2.1 Geometry and configuration

For the numerical analysis, the physical composite structural component of doubly curved laminated shell configuration has been modeled mathematically using the corresponding dimension i.e., the length 'a', width 'b' and thickness 'h'. Further, to maintain the numbers of layer, 'n'

arbitrarily oriented lamina is assumed with an arbitrary angle along the principal coordinates i.e., x_1 and x_2-axes refer to Fig. 1. The displacement field of the panel is based on the higher-order polynomial kinematics as shown in the following.

$$\begin{aligned} u(x_1,x_2,x_3,t) &= u_0(x_1,x_2,t) + x_3\theta_{x_1}(x_1,x_2,t) \\ &\quad + x_3^2\phi_{x_1}(x_1,x_2,t) + x_3^3\lambda_{x_1}(x_1,x_2,t) \\ v(x_1,x_2,x_3,t) &= v_0(x_1,x_2,t) + x_3\theta_{x_2}(x_1,x_2,t) \\ &\quad + x_3^2\phi_{x_2}(x_1,x_2,t) + x_3^3\lambda_{x_2}(x_1,x_2,t) \\ w(x_1,x_2,x_3,t) &= w_0(x_1,x_2,t) \end{aligned} \tag{1}$$

where, t is the time and u, v and w are the displacements of any point along the and coordinate axes respectively. u_0, v_0 and w_0, and are corresponding displacements of a point on the midplane and and are the rotations of normal to the mid-surface, i.e., $x_3 = 0$ about the x_1 and x_2-axes, respectively. The functions ϕ_{x_1}, ϕ_{x_2}, λ_{x_1} and λ_{x_2} are the higher order terms in the Taylor series expansion to maintain the parabolic variation of shear stress through the thickness of the panel.

The constitutive relation for any k^{th} (Fig. 2) lamina oriented at an arbitrary angle Θ about the principal material axes is expressed as

$$\{\sigma\} = [\bar{Q}]\{\varepsilon\} \tag{2}$$

The stress vector is formulated with the aid of the vector of forces

$$\{F\} = [D]\{\varepsilon\} \tag{3}$$

The elements of the stiffness matrix $[D]$ are defined as

$$[D] = \sum_{k=1}^{n} \int_{x_{3k-1}}^{x_{3k}} \left(\bar{Q}_{ij}\right)_k \left(1, x_3, x_3^2 \ldots. x_3^6\right) dx_3 \tag{4}$$

The strain vector of the laminated plate can be expressed as

$$\{\varepsilon\} = \begin{Bmatrix} \varepsilon_{x_1x_1} \\ \varepsilon_{x_2x_2} \\ \gamma_{x_1x_2} \\ \gamma_{x_1x_3} \\ \gamma_{x_2x_3} \end{Bmatrix} = \begin{Bmatrix} \dfrac{\partial u}{\partial x_1} + \dfrac{w}{R_{x_1}} \\ \dfrac{\partial v}{\partial x_2} + \dfrac{w}{R_{x_2}} \\ \dfrac{\partial u}{\partial x_2} + \dfrac{\partial v}{\partial x_1} + \dfrac{2w}{R_{x_1x_2}} \\ \dfrac{\partial u}{\partial x_3} + \dfrac{\partial w}{\partial x_1} - \dfrac{u}{R_{x_1}} \\ \dfrac{\partial v}{\partial x_3} + \dfrac{\partial w}{\partial x_2} \dfrac{v}{R_{x_2}} \end{Bmatrix} \tag{5}$$

2.2 Finite element formulation

The derived mathematical model order has been reduced for the computational purpose by using the displacement type FEM. In this regard, an isoparmetric nine noded element has been adopted to represent the structural kinematic model. After the necessary inclusion of the shape functions corresponding to the displacement vector "*d*" at any point on the mid-surface conceded to the following form

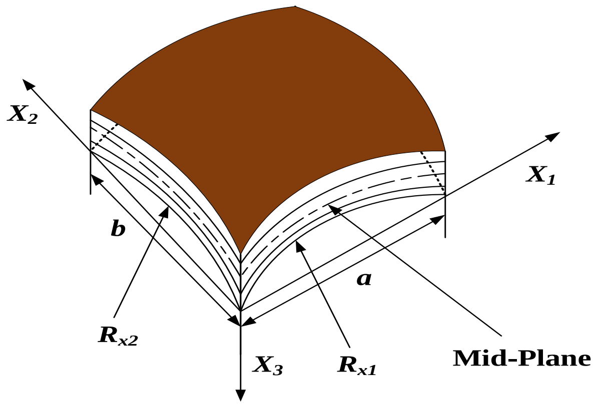

Fig. 1 Hybrid layered composite with geometrical details

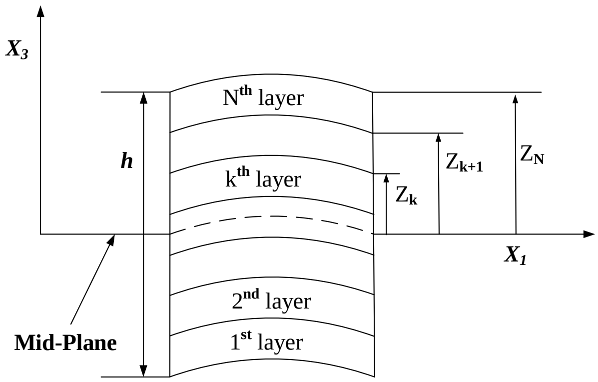

Fig. 2 Layer sequence and the thickness parameter

$$d = \sum_{i=1}^{n} N_i(x_1, x_2) d_i \tag{6}$$

where, the displacement i.e. $\{d\} = \left\{u_{0_i}\ v_{0_i}\ w_{0_i}?\theta_{x_{1_i}}\ \theta_{x_{2_i}}\ \phi_{x_{1_i}}\ \phi_{x_{2_i}}\ \lambda_{x_{1_i}}\ \lambda_{x_{2_i}}\right\}^T$ and shape functions (N_i) are defined for the i^{th} node.

Now, the modified mid-plane strain vector represented in matrix form as per the FEM implementation and conceded as

$$\{\varepsilon\} = [T]\{\bar{\varepsilon}\} \tag{7}$$

where, $[T]$ and $\{\bar{\varepsilon}\}$ are the corresponding thickness coordinate matrix and the mid-plane strain vectors and the equation once again reduced in to the following form

$$\{\varepsilon\} = [B_L]\{d_i\} \tag{8}$$

where, $[B_L]$ is a general linear type of strain displacement relation.

Moreover, the composite constitutive relations are expressed for any general laminated composite for any k^{th} lamina

$$\{\sigma\}^k = [Q]^k \{\varepsilon\}^k \tag{9}$$

where, $[Q]^k$, $\{\sigma\}^k$ and $\{\varepsilon\}^k$ are the reduced stress, total stress and strain vectors for the designated laminae.

Similarly, the total strain energy of the laminated panel has been expressed by implementing the stress and strain expression

$$U = \frac{1}{2}\iint\left[\int_{-h/2}^{+h/2} \{\varepsilon\}^T \{\sigma\} dx_3\right] dx_1 dx_2 \tag{10}$$

Now, Eq. (11) modified in to the following form to obtain the necessary equation

$$U = \frac{1}{2}\iint\left(\{\bar{\varepsilon}\}^T [D]\{\bar{\varepsilon}\}\right) dx_1 dx_2 \tag{11}$$

The total work done by an externally applied load, F is given by

$$W = \int_A \{\delta\}^T \{F\} dA \tag{12}$$

The elemental stiffness ($[k]$) can be further expressed as following

$$[k] = \int_A \left(\sum_{k=1}^{n} \int [B_L]^T [D][B_L] dx_3\right) dA \tag{13}$$

The transformations for the elemental stiffness and mass matrices of element can be expressed as

$$\left[\bar{k}\right] = [T]^T [k][T] \tag{14}$$

where, $\left[\bar{k}\right]$ is global stiffness matrix and the corresponding nodal displacement $\{d_i\}$ (i = 1, 4, 8) and $[k]$ is the elemental stiffness matrix of the laminated panel.

2.3 Governing equations

The final form of governing equation for bending analysis of laminated plate is obtained using variational principle

$$\delta\prod = \delta U - \delta W = 0 \tag{15}$$

where, δ is the variational symbol and $\prod$ represents the total potential energy.

The equilibrium equation for the flexural strength calculation of the hybrid composite panel obtained through substituting the relevant Eqs. i.e., (6), (11) and (12) into Eq. (16) and expressed as

$$[K]\{d\} = \{F\} \tag{16}$$

Finally, the Eq. (16) has been solved by utilizing the different sets of end conditions to avoid any further rigid body motion and to reduce total number of unknowns from the equation.

(*a*) Cenosphere (*b*) Epoxy and Hardener (*c*) Glass fibre (*d*) Release spray

Fig. 3 Raw materials used for fabrication hybrid cenosphere nanofiller Glass/Epoxy laminated composite

All sides simply-supported (SSSS)

$$\begin{aligned} &\text{at } x = 0 \text{ and } a \quad v_0 = w_0 = \theta_y = \phi_y = \lambda_y = 0 \ ; \\ &\text{at } y = 0 \text{ and } b \quad u_0 = w_0 = \theta_x = \phi_x = \lambda_x = 0 \end{aligned} \tag{17}$$

All sides clamped (CCCC)

$$\begin{aligned} &\text{at } x = 0 \text{ and } a;\ y = 0 \text{ and } b \\ &u_0 = v_0 = w_0 = \theta_x = \theta_y = \phi_x = \phi_y = \lambda_x = \lambda_y = 0 \end{aligned} \tag{18}$$

All sides free (FFFF)

$$\begin{aligned} &\text{at } x=0 \text{ and } a;\ y=0 \text{ and } b; \\ &u_0 \neq v_0 \neq w_0 \neq \theta_x \neq \theta_y \neq \phi_x \neq \phi_y \neq \lambda_x \neq \lambda_y \neq 0 \end{aligned} \tag{19}$$

3. Materials and method

3.1 Fabrication of composite

The raw materials required for the preparation of the glass cenosphere filled laminated composite i.e., nano glass cenosphere (Fig. 3(a)), woven glass fibre (Fig. 3(c)), epoxy and hardener (Fig. 3(b)) and polyvinyl alcohol release spray (Fig. 3(d)) can be seen in Fig. 3.

The hybrid composite plate filled with cenosphere type nanofiller composite prepared using the most common type of fabrication (hand layup) technique utilizing the different percentages of glass cenosphere. Initially, the woven glass fibres are cut into desired sizes for each kind of the composite plate fabrication and the matrix (epoxy) material mixed with cenosphere nanofiller in different percentages for a perfect mixture and the hardener added to the epoxy mixture with standard rule i.e., 10:1 ratio of weight percentage. Now, the glass fibre laminate is placed on the mylar sheet, which sprayed with polyvinyl alcohol spray and the epoxy mixture further added using a brush with adequate safety measure. The process has been repeated until the numbers of a layer need to be prepared. After completing the layups, one more mylar sheet with the release spray placed on the composite plate. Subsequently, a flat plate piece 50 kg of weight (approximately) placed above the prepared composite and allow for three days for the proper curing under the ambient condition. After the adequate curing, take out the laminated composite and for the preparation of the specimens according to the requirement i.e., tensile and flexural test.

3.2 Evaluation of material properties experimentally

The cenosphere filled glass/epoxy hybrid composite elastic material properties are tested experimentally through the universal testing machine (UTM), at CIPET Bhubaneswar. The specimen and the dimensional details are prepared according to internationally accepted standard i.e. ASTM D3039. The tensile test specimens are provided in Figs. 4(a) and 4(b) for before and after testing, respectively. The experimental properties (E_1, E_2 and E_{45}), for each specimen are recorded in all three required directions i.e. along the fibre length, perpendicular to fibre and at an angle 45^0 to fibre longitudinal direction. Additionally, the necessary shear properties of composite required for the analysis mainly calculated from the recorded modulus along the angular direction i.e., E_{45}. The experimental elastic properties also include Poison's ratio as 0.17 (Crawly 1979) according to the general practice. Also, to maintain the repeatability of the experimental properties, three different specimens for each case are tested and averaged to get the final material properties for all four different percentages of cenospheres laminated plates as shown in the Table 1. The following formulae (Jones 1975) is used to obtain the shear modulus of the Cenosphere filled Glass/Epoxy hybrid composite:

$$G_{12} = 1/\left(\frac{4}{E_{45}}\right) - \left(\frac{1}{E_1}\right) - \left(\frac{1}{E_2}\right) - \left(\frac{2\nu_{12}}{E_1}\right)$$

4. Results and discussion

After the fabrication and testing, the prepared in-house FE-MATLAB code has been utilized to compute the flexural responses of nano-cenosphere filled Glass/ Epoxy hybrid composite panels. The model consistency established via the well-known convergence analysis. Further, the presently obtained flexural deflections via the multiscale numerical model is compared with those of the published results to show the model validity. In addition, the different percentages of the nano-cenosphere filled Glass/ Epoxy laminated composite plate components are fabricated using the popular hand lay-up techniques for the lab-scale experimentation.

(a) Tensile specimen before test

(c) Bending specimen before test

(b) Tensile specimen after test

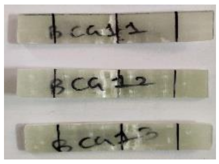

(d) Bending specimen after test

Fig. 4 Specimens before and after testing

(a) Tensile test

(b) Bending test

Fig. 5 Universal testing machines utilized for the property evaluation and deflection

Table 1 Experimentally evaluated material properties of different percentages of cenosphere

Nano Cenosphere (%)	E_1 (GPa)	G_{12} (GPa)	ν
Volume by 1%	8.438	2.9533	0.17
Volume by 2%	7.468	2.6138	0.17
Volume by 3%	7.338	2.5683	0.17
Volume by 4%	6.958	2.4353	0.17

The transverse mechanical bending deflections are obtained using the facility of National Institute of Technology Rourkela (NITR), Odisha, India, set up (universal testing machine). Also, the experimental deflection results are utilized for the comparison purpose with own numerical data obtained via the higher-order kinematic model. Also, the elastic properties utilized in the current analysis are obtained experimentally for different percentages of nanofiller filled composite. Finally, the effect variable parameters on the flexural deflections of the hybrid laminated structure computed to understand the effect of nanofiller on the curved panel structural responses.

4.1 Convergence and comparison study

In this section, the higher-order FE model consistency has been shown by the solving a specific numerical examples as same as the reference geometry, material and loading data (q_0 = 100 kN). The nondimensional deflection values of the simply-supported four layered cross ply [(0°/90°)$_2$] laminated composite are computed for three different geometries utilizing the given elastic property data i.e. graphite/epoxy lamina (Xiao *et al.* 2008) (E_1 = 250 GPa, E_2 = E_3 = 10 GPa, v_{12} = v_{23} = v_{13} = 0.25, G_{12} = G_{13} = 5 GPa, G_{23} = 2 GPa). The responses are calculated for different mesh densities and the corresponding deflections for three different geometries (R/a = 5, a/h = 50 and a/b =1) presented in Fig. 6. The figure indicates the convergence of the currently prepared home-made FE-MATLAB code for different mesh densities. Also, a (6×6) mesh is sufficient to compute the new responses and utilized further throughout the analysis.

4.2 Numerical validation

For the validation purpose, the nondimensional central deflection of the spherical structure with three different lamination scheme (0º/90º), (0º/90º/0º) and (0º/90º/90º/0º) is analyzed and compared with Reddy and Liu (1985). The geometrical and the material properties are taken as given in the reference. The current and reference central deflection responses are tabulated in Table 2 for the comparison purpose. From the table it can be understood that the results obtained using the proposed computer code and mathematical model are in good agreement with those of the reference values irrespective of the lamination scheme, curvature ratio and thickness ratio.

4.3 Comparison of numerical and experimental central deflection responses

The bending behavior, i.e., central deflection responses of different percentages of cenosphere nanofiller composites has been evaluated experimentally. For the investigation, the bending specimens are prepared following the instruction as given in the ASTMD 7264. The specimens are tested in UTM INSTRON-5967. The strain rate is kept constant (2 mm/min) throughout the test for the all specimens of each set. The responses are also calculated via present mathematical model and the comparison of the experimental and the numerical result is shown in Table 3.

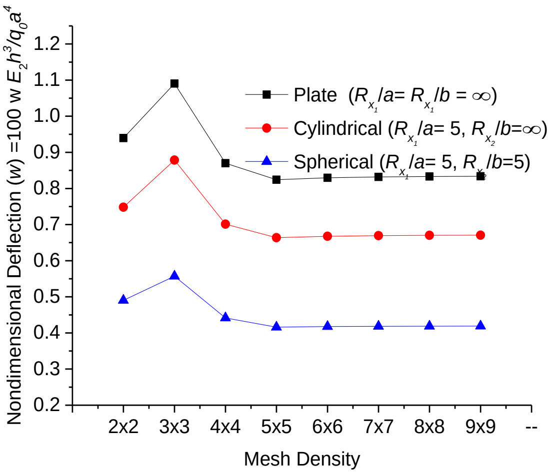

Fig. 6 Convergence behaviour of deflection including shell geometries

The table infers that the central deflection responses are increasing with the increasing the nanofiller percentage in composite. It is due to the decrease in Young's modulus values for different composite as provided in Table 1. It is interesting note that the responses are following an increasing path while the percentage of cenosphere increases in the composite matrix i.e., a decrement of elasticity has been observed both in property data and the deflections.

4.4 Numerical examples

The convergence including the validation indicates the suitability of the present proposed higher-order FE model for the prediction deflection of the nano-filler polymeric-hybrid composite component. Now, to show the model applicability, the transverse deflection values are computed using the customized computer code for different structural design-dependent parameters under the influence of 100 N mechanical transverse loading (uniformly distributed type), if not stated otherwise. The bending strength and corresponding inferences from the numerical examples are discussed for each case.

4.4.1 Effect of aspect ratio (a/b)

In this example, the transverse bending values are computed for simply supported four-layers thin (a/h = 50) cylindrical shell structure (R/a= 40) by varying the aspect ratios (like a/b =1, 1.5, 2, 2.5 and 3). The variation of flexural nondimensional deflections of the composite is obtained for all four types of cenosphere filled hybrid composite utilizing the experimental elastic data under 100N mechanical transverse loading (refer to Fig. 7).

It can be concluded from the results that the nondimensional deflections of the structure are increasing when the aspect ratio increases regardless of the cenosphere fraction in the hybrid composite. Also, the deflection values are increasing for all four composites i.e., Composite-1 to Composite-4 (Composite-1 <Composite-2 <Composite-3 <Composite-4) due to the decrement in elastic modulus of the hybrid composite.

Table 2 Validation study nondimensional central deflection responses of spherical shell panel

R/*a*	Model	0º/90º		0º/90º/0º		0º/90º/90º/0º	
		a/*h*=100	*a*/*h* =10	*a*/*h* =100	*a*/*h* =10	*a*/*h* =100	*a*/*h* =10
50	Source (FSDT)	15.714	19.452	6.4827	10.214	6.6148	10.245
	Source (HSDT)	15.711	19.155	6.4895	10.893	6.6234	11.049
	Present	15.734	19.479	6.5716	11.117	6.6925	11.267
100	Source (FSDT)	16.645	19.464	6.6421	10.218	6.7772	10.249
	Source (HSDT)	16.642	19.168	6.6496	10.898	6.7866	11.053
	Present	16.662	19.492	6.7341	11.121	6.8576	11.271
∞	Source (FSDT)	16.98	19.469	6.697	10.22	6.8331	10.251
	Source (HSDT)	16.977	19.172	6.7047	10.899	6.8427	11.055
	Present	16.997	19.497	6.79	11.122	6.9145	11.272

Table 3 Comparison of Numerical and Experimental central deflection responses

Load (N)	Central deflections (mm)							
	Composite-1		Composite-2		Composite-3		Composite-4	
	Nu	Ex	Nu	Ex	Nu	Ex	Nu	Ex
15	0.0318	0.0337	0.0359	0.3963	0.0366	0.03987	0.0386	0.04169
30	0.0636	0.0674	0.0719	0.07749	0.0732	0.07805	0.0772	0.08186
45	0.0954	0.1011	0.1078	0.11421	0.1098	0.11602	0.1158	0.12119
60	0.1273	0.1348	0.1438	0.15007	0.1463	0.15419	0.1543	0.16157
75	0.1591	0.1685	0.1797	0.18723	0.1829	0.19205	0.1929	0.20079
90	0.1909	0.2022	0.2157	0.22324	0.2195	0.23068	0.2315	0.23987

Nu: Numerical, Ex: Experimental

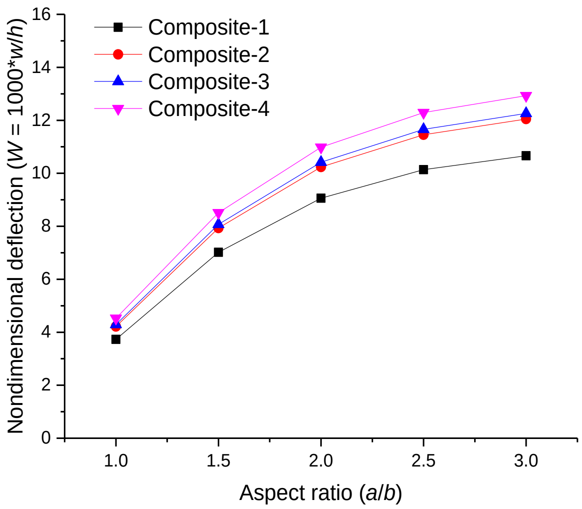

Fig. 7 Effect of aspect ratio on flexural analysis for simply supported symmetric cylindrical shell structured composite (R/a = 40 and a/h = 50)

4.4.2 Effect of end conditions on deflection data

In this example, a thin (a/h = 40) square (a/b = 1) elliptical panel (R/a = 50) flexural analysis of a laminated elliptical shell is utilized for the mechanical bending analysis for one or more combinations of end conditions (CCCC, SCSC, CFCF, SSSS, SFSF and CFFF) under the uniformly distributed loading (100 N). The nondimensional deflections of differently filled composite and support conditions are conceded in Fig. 8. The deflection data follow the expected line i.e., increasing while the number of constraint and modulus of elasticity values is decreasing (composite type 1 to 4, the weight fractions of cenosphere increases and the elastic modulus decreases subsequently).

4.4.3 Deflection of different geometrical configurations

The effect of geometrical configurations largely affects the structural strength and stiffness, the current example solved to show the effect based on their deflection parameter. For the numerical part, a square (a/b = 1), thin (a/h = 50) composite cross-ply shallow (R/a = 40) shell panel problem has been solved under the influence of uniformly distributed type mechanical transverse (q_0 = 100 N) loading. The variation of the transverse flexural deflection data provided in Fig. 9 for the different composite of variable weight fractions of filler material and five different geometrical configurations (cylindrical, hyperboloid, elliptical, spherical and plate). The responses are showing minimum for the spherical panel and composite type 1, i.e., the lowest weight fractions of filler. This is because the load line flows smoothly for the spherical panel due to the curvature continuity.

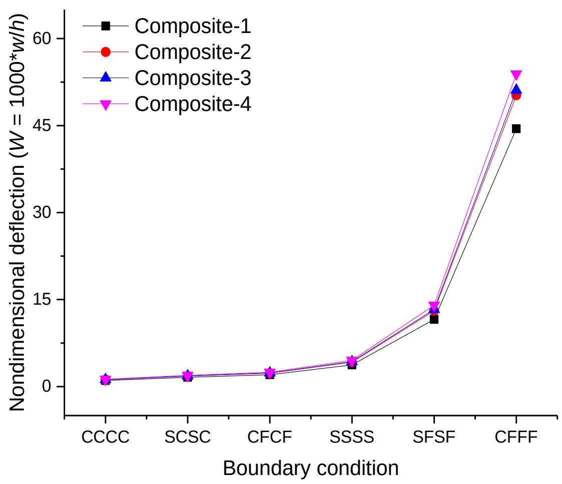

Fig. 8 Effect of end constraint on flexural strength symmetric angle-ply elliptical shell (R/a = 40, a/b = 1 and a/h = 50)

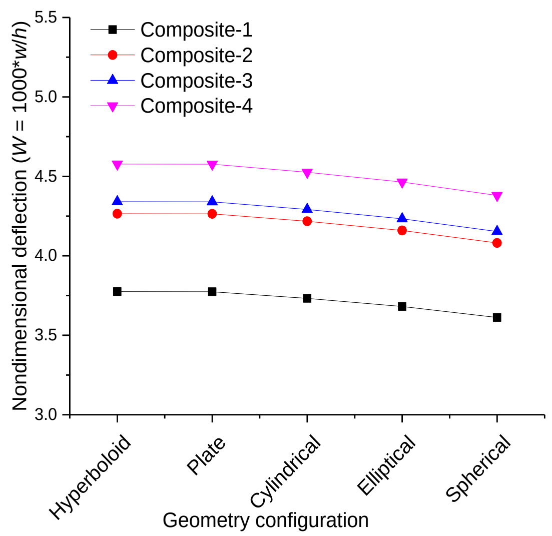

Fig. 9 Configurational effect on flexural strength for simply-supported four layer cross-ply composite structure (R/a = 40, a/b = 1 and a/h = 50)

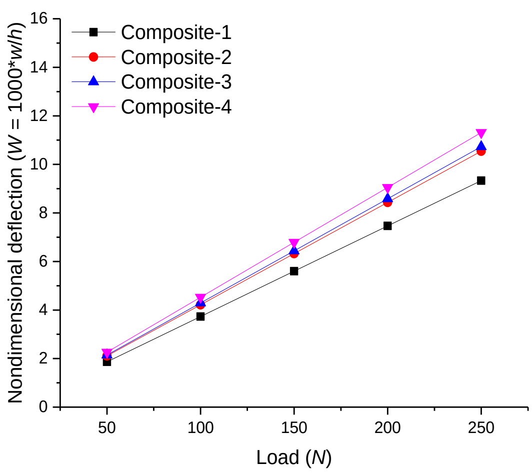

Fig. 10 Load intensity effect on flexural deflection of simply-supported cross-ply cylindrical panel (R/a = 40, a/b = 1 and a/h = 50)

4.4.4 Effect of loading intensity

The structural deflection directly proportional to the loading intensity and the same has been obtained in this example considering a cylindrical panel geometry of variable elastic properties for different cenosphere filled composite. The numerical data are obtained for the thin (a/h = 50), square (a/b = 1) simply supported antisymmetric cross-ply panel under five load intensities (q_0 = 50, 100, 150, 200 and 250 N) and shown in Fig. 10. From the results, it can be understood that the nondimensional deflections of the panel are increasing when the loading increases gradually irrespective of the cenosphere weight percentage.

4.4.5 Curvature ratio (R/a) influence on deflection parameter

In this example, the central deflections of the cenosphere filled composite spherical shell structure are computed using the experimental properties for five curvature ratios (R/a = 10, 20, 30, 50 and 80). The responses are evaluated by adopting other geometrical parameters as, a/b = 1 and a/h = 50 under the influence of 100 N mechanical loadings and presented in Fig. 11. The results follow a similar pattern as in the earlier case i.e., the stiffer and flexible configurations are Composite-1 and Composite-4, respectively. Additionally, the deflection values are following an increasing line when the curvature ratio increases. This is because the curved panel structural component possesses higher stretching energy in comparison to the bending when compared to flat panel.

5. Conclusions

The flexural deflections of the nano cenosphere filled glass/epoxy hybrid laminated composite panel are computed numerically using a higher-order FE model with the help of an in-house MATLAB code. The finite element solution validity of the glass/epoxy composite is examined with available published benchmark solutions. Also, the numerical model verified with own experimental deflection values by preparing four different volume fractions of

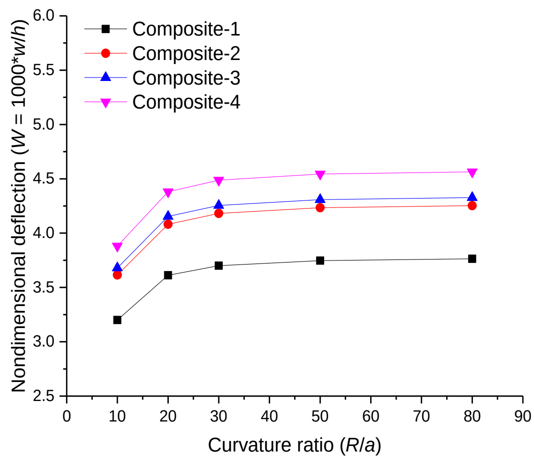

Fig. 11 Deflection responses due to variable curvature ratio of simply-supported symmetric cross-ply spherical shell panel (a/h = 50 and a/b = 1)

cenosphere filled glass-epoxy composite. Moreover, the current finite element and experimental deflections are simulated using the experimental material data i.e., experimental elastic properties of the different hybrid composite (cenosphere filled with different weight fractions). Based on the numerical and subsequent experimental verification, the model has been extended to obtain the responses for the variable important geometrical parameter, loading intensity and geometrical configuration adopted for the structural design. The responses are simulated numerically using the experimental elastic properties of all four kinds of hybrid composite and the corresponding conclusions listed in the point-wise fashion in the following lines.

- The numerical model responses are compared with available published data for different kind of kinematic models, curvature parameter (shallow) and thickness ratios (moderately thick and thin) to establish the accuracy including the consistency provided via the convergence study.
- The model results are also verified with own experimental data by preparing in-house hybrid composite for different volume fractions of nano cenosphere and the corresponding experimental properties utilized throughout the analysis.
- The experimental elastic properties indicate the decrement of the elastic moduli with the increase of nano-cenosphere filler volume percentage. This, in turn, reduces the structural stiffness and the increases deflection values.
- In general, the deflection parameter is increasing while the weight percentage of cenosphere increases in the composite constituent irrespective of the individual parameter. However, the spherical panel shows the stiffest configuration while compared to other geometries irrespective of the cenosphere weight fractions.

References

Amnieh, H.B., Zamzam, M.S. and Kolahchi, R. (2018), "Dynamic analysis of non-homogeneous concrete blocks mixed by SiO2 nanoparticles subjected to blast load experimentally and theoretically", *Constr. Build. Mater.*, **174**, 633-644. https://doi.org/10.1016/j.conbuildmat.2018.04.140.

Arani, A.G., Cheraghbak, A. and Kolahchi, R. (2016a), "Dynamic buckling of FGM viscoelastic nano-plates resting on orthotropic elastic medium based on sinusoidal shear deformation theory", *Struct. Eng. Mech.*, **60**(3), 489-505. http://dx.doi.org/10.12989/sem.2016.60.3.489.

Arani, A.G., Jafari, G.S. and Kolahchi, R. (2016b), "Vibration analysis of nanocomposite micro plates integrated with sensor and actuator layers using surface SSDPT", *Polymer Compos.*, **39**(6), 1936-1949. https://doi.org/10.1002/pc.24150.

Arencon, D., Velasco, J.I., Realinho, V., Sanchez-Soto, M. and Gordillo, A. (2007), "Fracture toughness of glass microsphere-filled polypropylene and polypropylene/poly (ethylene terephthalate-co-isophthalate) blend-matrix composites", *J. Mater, Sci.*, **42**(1), 19-29. https://doi.org/10.1007/s10853-006-1036-1.

Asadi, H. and Beheshti, A. R. (2018), "On the nonlinear dynamic responses of FG-CNTRC beams exposed to aerothermal loads using third-order piston theory", *Acta Mechanica*, **229**(6), 2413-2430. https://doi.org/10.1007/s00707-018-2121-7

Bellifa, H., Benrahou, K.H., Hadji, L., Houari, M.S.A. and Tounsi, A. (2016), "Bending and free vibration analysis of functionally graded plates using a simple shear deformation theory and the concept the neutral surface position", *J. Brazilian Soc. Mech. Sci. Eng.*, **38**(1), 265-275. https://doi.org/10.1007/s40430-015-0354-0

Corigliano, A., Rizzi, E. and Papa, E. (2000), "Experimental characterization and numerical simulations of a syntactic-foam/glass-fibre composite sandwich", *Compos. Sci. Technol.*, **60**(11), 2169-2180. https://doi.org/10.1016/S0266-3538(00)00118-4

Crawley, E.F. (1979), "The natural modes of graphite/epoxy cantilever plates and shells", *J. Compos. Mater.*, **13**(3), 195-205. https:doi.org/10.1177/002199837901300302.

Dombrovsky, L.A., Randrianalisoa, J.H. and Baillis, D. (2007), "Infrared radiative properties of polymer coatings containing hollow microspheres", *Int. J. Heat Mass Transfer*, **50**(7-8), 1516-1527. https://doi.org/10.1016/j.ijheatmasstransfer. 2006.08.034.

Doumbia, A.S., Bourmaud, A., Jouannet, D., Falher, T., Orange, F., Retoux, R. and Cauret, L. (2015), "Hollow microspheres–poly-(propylene) blends: Relationship between microspheres degradation and composite properties", *Polymer Degradation Stability*, **114**, 146-153. https://doi.org/10.1016/j.polymdegradstab.2014.12.024.

Esmaeili, H.A., Ghaitani, M .M and Kolahchi, R. (2014), "Oil and Gas Pipes Reinforced with Carbon Nanotubes: Bending Analysis". *International Conference on Civil, Biological and Environmental Engineering* (CBEE-2014) May 27-28, 2014 Istanbul (Turkey) https://doi.org/10.1016/j.jmatprotec.2006.03.104.

Ferreira, J.A.M., Capela, C. and Costa, J.D. (2010), "A study of the mechanical behaviour on fibre reinforced hollow microspheres hybrid composites", *Compos. Part A: Appl. Sci. Manufact.*, **41**(3), 345-352. https://doi.org/10.1016/j.compositesa.2009.10.018.

Ghannadpour, S.A.M. (2018), "Ritz method application to bending, buckling and vibration analyses of timoshenko beams via nonlocal elasticity", *J. Appl. Comput. Mech.*, **4**(1), 16-26. DOI: 10.22055/JACM.2017.21915.1120.

GhannadPour, S.A.M. and Alinia, M.M. (2006), "Large deflection behavior of functionally graded plates under pressure loads", *Compos. Struct.*, **75**(1-4), 67-71. https://doi.org/10.1016/j.compstruct.2006.04.004.

Ghannadpour, S.A.M., Mohammadi, B. and Fazilati, J. (2013), "Bending, buckling and vibration problems of nonlocal Euler beams using Ritz method", *Compos. Struct.*, **96**, 584-589. https://doi.org/10.1016/j.compstruct.2012.08.024.

Gupta, N. and Nagorny, R. (2006), "Tensile properties of glass microballoon-epoxy resin syntactic foams", *J. Appl. Polymer Sci.*, **102**(2), 1254-1261. https://doi.org/10.1002/app.23548.

Hajmohammad, M.H., Azzizkhani, M.B. and Kolahchi, R. (2018c), "Multiphase nanocomposite viscoelastic laminated conical shells subjected to magneto-hygrothermal loads: Dynamic buckling analysis", *Int. J. Mech. Sci.*, **137**, 205-213. https://doi.org/10.1016/j.ijmecsci.2018.01.026.

Hajmohammad, M.H., Farrokhian, A. and Kolahchi, R. (2018b), "Smart control and vibration of viscoelastic actuator-multiphase nanocomposite conical shells-sensor considering hygrothermal load based on layerwise theory", *Aerosp. Sci.Technol.*, **78**, 260-270. https://doi.org/10.1016/j.ast.2018.04.030.

Hajmohammad, M.H., Zarei, M.S., Farrokhian, A. and Kolahchi, R. (2018a), "A layerwise theory for buckling analysis of truncated conical shells reinforced by CNTs and carbon fibers integrated with piezoelectric layers in hygrothermal environment", *Adv. Nano Res.*, **6**(4), 299-321. https://doi.org/10.12989/anr.2018.6.4.299.

Heydari, M.M., Kolahchi, R., Heydari, M. and Abbasi, A. (2014), "Exact solution for transverse bending analysis of embedded laminated Mindlin plate", *Struct. Eng. Mech.*, **49**(5), 661-672. http://dx.doi.org/10.12989/sem.2014.49.5.661.

Jassas, M.R., Bidgoli, M.R. and Kolahchi, R. (2019), "Forced vibration analysis of concrete slabs reinforced by agglomerated SiO2 nanoparticles based on numerical methods", *Constr. Build. Mater.*, **211**, 796-806. https://doi.org/10.1016/j.conbuildmat.2019.03.263.

Jones, R.M. (1975), Mechanics of Composite Materials, Taylor & Francis, Philadelphia.

Kang, D., Hwang, S.W., Jung, B.N. and Shim, J.K. (2017), "Effect of hollow glass microsphere (HGM) on the dispersion state of single-walled carbon nanotube (SWNT", *Compos. Part B: Eng.*, **117**, 35-42. https://doi.org/10.1016/j.compositesb.2017.02.038.

Kempf, U.W. (2000), U.S. Patent No. 6,042,936. Washington, DC: U.S. Patent and Trademark Office.

Kolahchi, R., Bidgoli, A.M.M. and Heydari, M.M. (2015), "Size-dependent bending analysis of FGM nano-sinusoidal plates resting on orthotropic elastic medium", *Struct. Eng. Mech.*, **55**(5), 1001-1014. http://dx.doi.org/10.12989/sem.2015.55.5.1001.

Kolahchi, R., Hosseini, H., Fakhar, M.H., Taherifar, R. and Mahmoudi, M. (2019), "A numerical method for magneto-hygro-thermal postbuckling analysis of defective quadrilateral graphene sheets using higher order nonlocal strain gradient theory with different movable boundary conditions", *Comput. Math. Appl.,* **78**(6), 2018-2034. https://doi.org/10.1016/j.camwa.2019.03.042.

Kumar, N., Mireja, S., Khandelwal, V., Arun, B. and Manik, G. (2017), "Light-weight high-strength hollow glass microspheres and bamboo fiber based hybrid polypropylene composite: A strength analysis and morphological study", *Compos. Part B: Eng.*, **109**, 277-285. https://doi.org/10.1016/j.compositesb.2016.10.052.

Li, J., Luo, X. and Lin, X. (2013), "Preparation and characterization of hollow glass microsphere reinforced poly (butylene succinate) composites", *Mater. Design*, **46**, 902-909. https://doi.org/10.1016/j.matdes.2012.11.054.

Liang, J.Z. and Li, R. K. Y. (2000), "Effect of filler content and surface treatment on the tensile properties of glass-bead-filled polypropylene composites", *Polymer Int.*, **49**(2), 170-174. https://doi.org/10.1002/(SICI)1097-0126(200002)49.

Ovesy, H.R. and Ghannadpour, S (2009), "An exact finite strip for the calculation of relative post-buckling stiffness of isotropic plates", *Struct. Eng. Mech.*, **31**(2), 181-210. http://dx.doi.org/10.12989/sem.2009.31.2.181.

Ovesy, H.R. and Ghannadpour, S.A.M. (2006), "Large deflection behavior of functionally graded plates under pressure loads, using finite strip method", *Proceedings of the 3rd European Conference on Computational Mechanics* (pp. 697-697). https://doi.org/10.1007/1-4020-5370-3_697.

Reddy, J.N. and Liu, C.F. (1985), "A higher-order shear deformation theory of laminated elastic shells" *Int. J. Eng. Sci.*, **23**(3), 319-330.

Taghizadeh, M., Ovesy, H.R. and Ghannadpour, S.A.M. (2015), "Nonlocal integral elasticity analysis of beam bending by using finite element method", *Struct. Eng. Mech.*, **54**(4), 755-769. http://dx.doi.org/10.12989/sem.2015.54.4.755.

Wang, J., Liang, G., He, S. and Yang, L. (2010), "Curing behavior and mechanical properties of hollow glass microsphere/bisphenol a dicyanate ester composites", *J. Appl. Polymer Sci.*, **118**(3), 1252-1256. https://doi.org/10.1002/app.32446.

Wang, L., Yang, X., Zhang, J., Zhang, C. and He, L. (2014), "The compressive properties of expandable microspheres/epoxy foams", *Compos. Part B: Eng.*, **56**, 724-732. https://doi.org/10.1016/j.compositesb.2013.09.030.

Wu, X., Dong, L., Zhang, F., Zhou, Y., Wang, L., Wang, D. and Yin, Y. (2016), "Preparation and characterization of three phase epoxy syntactic foam filled with carbon fiber reinforced hollow epoxy macrospheres and hollow glass microspheres", *Polymer Compos.*, **37**(2), 497-502.

Xiao, J.R., Gilhooley, D.F., Batra, R.C., Gillespie Jr. J.W. and McCarthy, M.A. (2008), "Analysis of thick composite laminates using a higher-order shear and normal deformable plate theory (HOSNDPT) and a meshless method", *Compos. Part B: Eng.*, **39**(2), 414-427. https://doi.org/10.1016/j.compositesb.2006.12.009.

Yung, K.C., Zhu, B.L., Yue, T.M. and Xie, C.S. (2009), "Preparation and properties of hollow glass microsphere-filled epoxy-matrix composites", *Compos. Sci. Technol.*, **69**(2), 260-264. https://doi.org/10.1016/j.compscitech.2008.10.014.

Zamanian, M., Kolahchi, R. and Bidgoli, M.R. (2017), "Agglomeration effects on the buckling behaviour of embedded concrete columns reinforced with SiO2 nano-particles", *Wind Struct.*, **24**(1), 43-57. http://dx.doi.org/10.12989/was.2017.24.1.043.

Zhang, L. and Ma, J. (2010), "Effect of coupling agent on mechanical properties of hollow carbon microsphere/phenolic resin syntactic foam", *Compos. Sci. Technol.*, **70**(8), 1265-1271. https://doi.org/10.1016/j.compscitech.2010.03.016.

Zhang, L. and Ma, J. (2013), "Effect of carbon nanofiber reinforcement on mechanical properties of syntactic foam", *Mater. Sci. Eng.*: A, **574**, 191-196. https://doi.org/10.1016/j.msea.2013.03.028.

Zhu, B.L., Zheng, H., Wang, J., Ma, J., Wu, J. and Wu, R. (2014), "Tailoring of thermal and dielectric properties of LDPE-matrix composites by the volume fraction, density, and surface modification of hollow glass microsphere filler", *Compos.Part B: Eng.*, **58**, 91-102. https://doi.org/10.1016/j.compositesb.2013.10.029.

Zidi, M., Tounsi, A., Houari, M.S.A. and Bég, O.A. (2014), "Bending analysis of FGM plates under hygro-thermo-mechanical loading using a four variable refined plate theory", *Aerosp. Sci. Technol.*, **34**, 24-34. https://doi.org/10.1016/j.ast.2014.02.001.

CC